Quaternary Science Reviews 29 (2010) 3875–3886

Contents lists available at ScienceDirect

Quaternary Science Reviews

journal homepage: www.elsevier.com/locate/quascirev

Phase relationships of North Atlantic ice-rafted debris and surface-deep climate proxies during the last glacial period

David A. Hodell [a,*], Helen F. Evans [b], James E.T. Channell [c], Jason H. Curtis [c]

[a] Godwin Laboratory for Paleoclimate Research, Department of Earth Sciences, University of Cambridge, Downing Street, Cambridge CB2 3EQ, UK
[b] Borehole Research Group, Lamont-Doherty Earth Observatory of Columbia University, 61 Route 9W, Palisades, NY 10964, USA
[c] Department of Geological Sciences, University of Florida, P.O. Box 112120, Gainesville, FL 32611, USA

ARTICLE INFO

Article history:
Received 15 January 2010
Received in revised form
28 August 2010
Accepted 8 September 2010

ABSTRACT

We report stable isotope, core scanning XRF, and ice-rafted detritus (IRD) data in glacial-aged sediments from piston Core KN166-14-JPC-13 (hereafter referred to as JPC-13) retrieved at 53.1°N 33.5°W on the southern Gardar Drift, North Atlantic. A chronology was established by correlating millennial-scale features in the benthic $\delta^{18}O$ record to Portuguese Margin Core MD95-2042. Once the alignment of benthic $\delta^{18}O$ of JPC-13 to MD95-2042 is fixed, the relative timing of proxy variables is used to determine the phasing of changes in IRD and surface-deep hydrography. Each peak in North Atlantic IRD coincided with a decrease in benthic $\delta^{18}O$ that, in turn, has been linked to warming in Antarctica (Events A1–A7). The IRD pulses are followed shortly thereafter by abrupt decreases in planktonic $\delta^{18}O$, indicating warming and increased heat transport to the subpolar North Atlantic associated with Greenland interstadials (GIS) 8, 12,14, and 16–17. Grain-size and elemental (*K*/Ti) variations indicate that Iceland–Scotland Overflow Water (ISOW) was stronger during these long, warm interstadial periods of Marine Isotope Stage (MIS) 3. The results are consistent with interhemispheric phase relationships inferred from Iberian Margin sediment cores and with methane synchronization of Greenland and Antarctic ice cores.

1. Introduction

Millennial-scale climate variability during the last glacial period has a somewhat different character between Greenland and Antarctica. Greenland ice cores display abrupt stadial–interstadial oscillations resembling a 'square-wave' form (Dansgaard–Oeschger (D–O) events), whereas Antarctic ice cores show a 'triangular' form consisting of Antarctic Isotope Maxima [AIM] that are accompanied by variations in atmospheric CO_2 (Indermühle et al., 2000; Ahn and Brook, 2008). The Greenland D–O events are bundled into longer-term packages, with the beginning of the cycle marked by warming and the end of the cycle marked by Heinrich events (Heinrich, 1988; Bond et al., 1993). This pattern, sometimes referred to as a Bond cycle, is similar in time scale to the major features of Antarctic climate variability albeit phase shifted.

Studying the phase relationships of millennial-scale variability is important for determining the relative timing among various processes in the climate system. The interhemispheric phasing for the last 90 kyrs has been determined by synchronizing methane records between Greenland and Antarctic ice cores (Blunier and Brook, 2001; EPICA Community Members, 2006). Results indicate that the warm events in Antarctica coincided with the longest, coldest stadials in Greenland associated with Heinrich events. The Heinrich stadials were immediately followed by abrupt warming in Greenland resulting in a long interstadial period at the same time as Antarctica began to cool. The phasing between Greenland and Antarctica has been described as either anti-phase ("seesaw") or phase shifted ("Southern lead"), although neither description adequately captures the complexity of the phase relationship (Steig and Alley, 2002). The out-of-phase behavior has been attributed to the "bipolar seesaw" whereby changes in heat transport related to Atlantic Meridional Overturning Circulation (AMOC) results in a warming (cooling) in the north and cooling (warming) in the south when AMOC is strong (weak) (Mix et al., 1986; Crowley, 1992; Broecker, 1998; Stocker, 1998; Stocker and Johnsen, 2003; Knutti et al., 2004). The amplitude of Antarctic warm events shows a linear relationship with the duration of the accompanying stadial periods in Greenland during MIS3 (EPICA Community Members, 2006).

Determining phase relationships of millennial-scale variability in glacial periods beyond the last climate cycle is challenging because Greenland ice cores are presently limited to the last

* Corresponding author. Tel.: +44 0 1223 330270; fax: +44 0 1223 333450.
E-mail address: dah73@cam.ac.uk (D.A. Hodell).

0277-3791/$ – see front matter Crown Copyright © 2010 Published by Elsevier Ltd. All rights reserved.
doi:10.1016/j.quascirev.2010.09.006

124 kyr. Absolute dating of marine cores is too imprecise to correlate and resolve small differences in the timing of paleoclimate signals (Andrews et al., 1999; Wunsch, 2006). An alternative approach is to determine the relative phasing of changes in proxy variables in the same core that monitor different components of the ocean-climate system. Despite the merits of inferring phase relationships in a single core, caution is needed because bioturbation combined with changes in species abundances and sedimentation rates can affect lead/lag relationships among proxy variables in the same core (Löwemark and Grootes, 2004; Löwemark et al., 2008).

One of the first studies to apply this technique was Charles et al. (1996) who compared planktonic $\delta^{18}O$ and benthic $\delta^{13}C$ in South Atlantic Core RC11-83 and concluded that northern hemisphere climate change lagged those of the southern hemisphere by 1500 years. This result was later confirmed by methane synchronization of polar ice cores (Blunier et al., 1998, Blunier and Brook, 2001; EPICA Community Members, 2006).

Shackleton et al. (2000, 2004) produced a detailed planktonic $\delta^{18}O$ record of millennial-scale variability in Portuguese Margin Core MD95-2042 that can be confidently correlated to Greenland ice cores. The benthic $\delta^{18}O$ signal in the same core resembles temperature records from Antarctic ice cores, although the cause of this correlation is not well understood. Changes in benthic $\delta^{18}O$ may in large part reflect local deep-water $\delta^{18}O_{dw}$, related to changes in deep-water sourcing and/or source signature (Skinner et al., 2007). Shackleton et al. (2000, 2004) correlated the planktic $\delta^{18}O$ of MD95-2042 to Greenland and used methane synchronization of polar ice cores to evaluate the phase relationship with Antarctica (Blunier et al., 1998; Blunier and Brook, 2001; EPICA Community Members, 2006). They found the relative timing of the planktonic and benthic $\delta^{18}O$ signals has the same interhemispheric phasing as that deduced from other studies (Blunier et al., 1998, Blunier and Brook, 2001); that is, millennial-scale warmings in Antarctica preceded the onset of Greenland warmings and the onset of rapid warming in Greenland coincided with cooling in Antarctica (Charles et al., 1996; Blunier et al., 1998, Blunier and Brook, 2001; EPICA Community Members, 2006).

Following the lead of previous investigators (Charles et al., 1996; Shackleton et al., 2000), we applied a similar strategy to study phase relationships of multi-proxy data from piston core KN166-14-JPC-13 (hereafter referred to as JPC-13) located on the southern Gardar Drift in the subpolar North Atlantic (Fig. 1). A precise chronology (SFCP04) was established by correlating millennial-scale features in the benthic $\delta^{18}O$ record of JPC-13 to Portuguese Margin Core MD95-2042 (Fig. 2) that, in turn, has been synchronized with Greenland and Antarctic ice cores (Shackleton et al., 2004). By comparing the relative timing of proxy variables in JPC-13 relative to the benthic $\delta^{18}O$ signal, we infer the phasing of changes in surface and bottom water hydrography and their relation to delivery of ice-rafted debris (IRD) to the subpolar North Atlantic. The focus of the paper is on the last 80 ka because this is the period for which the common SFCP04 time scale is available for Iberian Margin Core MD95-2042 and ice cores from Greenland (GRIP) and Antarctica (Vostok) (Shackleton et al., 2004).

2. Site location and hydrography

A 23.6-m piston core (KN166-14-13JPC) was recovered in 2002 from the southernmost Gardar Drift near the Charlie Gibbs Fracture Zone (53° 3.41′, 33° 31.78′, 3082 m). The Gardar Drift is an elongated contourite deposited along the eastern flank of the Reykjanes Ridge, which formed by the interaction of Iceland–Scotland Overflow Water (ISOW), flowing as a Deep Western Boundary Current (DWBC), and local topography (Bianchi and McCave, 2000). During the last glaciation, JPC-13 was located a few degrees north of the "Ruddiman IRD belt" (Ruddiman, 1977; Robinson et al., 1995) (Fig. 1). The site is at 3082 m water depth and is bathed today by

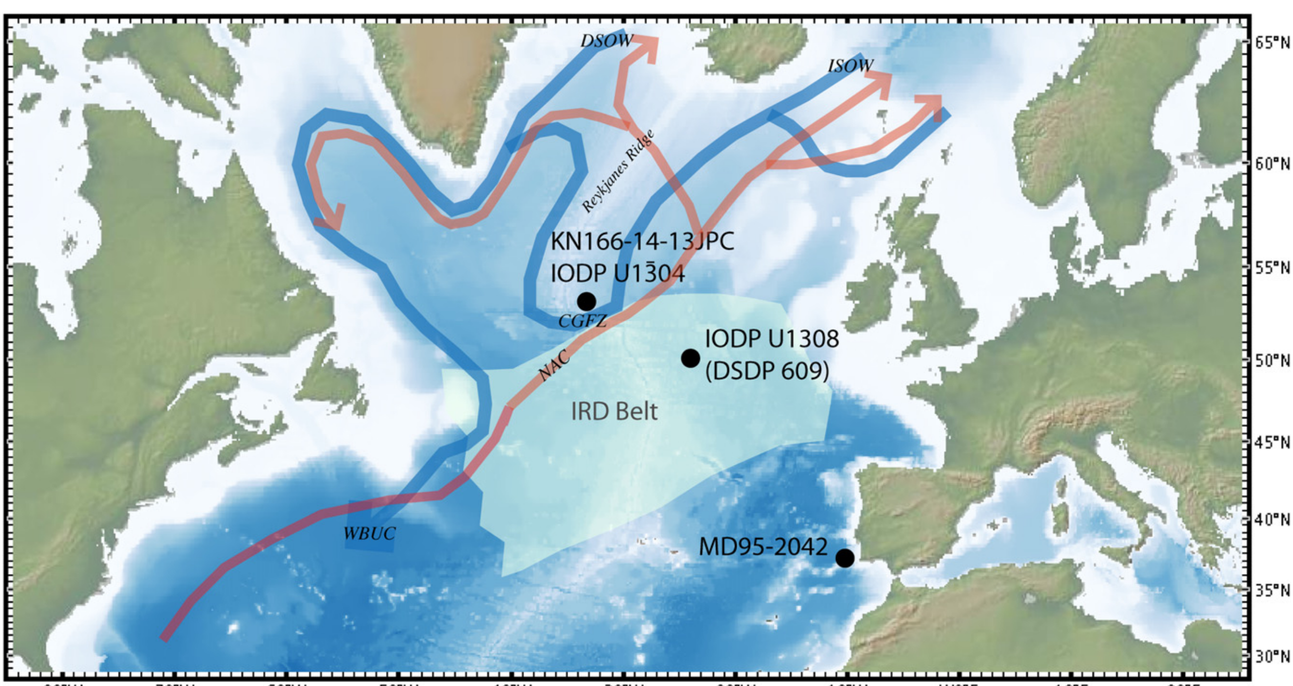

Fig. 1. Site location of Cores KN1666-14-JPC-13 (IODP Site U1304), MD95-2042, and IODP Site U1308 in the North Atlantic. Surface currents (red lines) and deep currents (blue lines) represent a schematic illustration of the major components of the Atlantic Meridional Overturning Circulation (AMOC). Light blue shaded area represents the approximate position of the IRD belt during the last glacial period (Ruddiman, 1977). Red lines represent the idealized surface water and dark blue lines the deep-water limbs of AMOC. ISOW = Iceland–Scotland Overflow Water; DSOW = Denmark Strait Overflow Water; WBUC = Western Boundary Undercurrent; CGFZ = Charlie Gibbs Fracture Zone; NAC = North Atlantic Current. (For interpretation of the references to colour in this figure legend, the reader is referred to the web version of this article.)

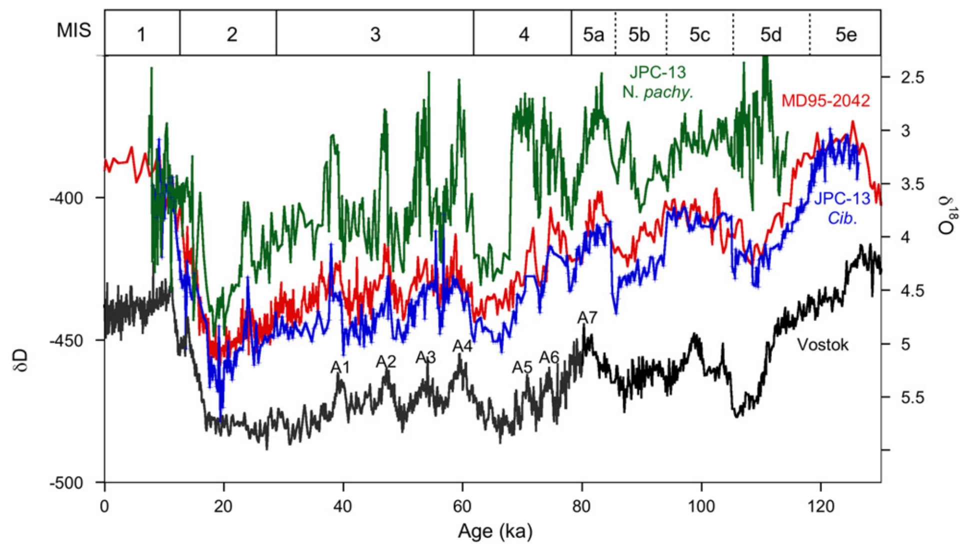

Fig. 2. Stratigraphic overview of Core JPC-13 showing $\delta^{18}O$ records of *C. wuellerstorfi* (blue) and *N. pachyderma* (green). Specimens of *N. pachyderma* (sin) are too rare for oxygen isotope analysis during the full interglacial conditions of the Holocene and MIS 5e. The chronology of JPC-13 was derived by correlating the benthic $\delta^{18}O$ of JPC-13 (blue) to MD95-2042 (red) to 80 ka and to LRO4 thereafter (Lisiecki and Raymo, 2005). Also shown for comparison is the Vostok δD record (gray) with Antarctic warm events labeled (A1–A7). (For interpretation of the references to colour in this figure legend, the reader is referred to the web version of this article.)

a mixture of ISOW and Lower Deep-Water (LDW), with the latter containing water sourced from the Southern Ocean. ISOW transports approximately 6 sverdrups of water through the CGFZ (Smethie et al., 2007) and, together with Labrador Sea Water and Denmark Strait Overflow Water, constitutes the primary components of North Atlantic Deep-Water (NADW).

3. Materials and methods

U-channel samples (1.8 cm × 1.9 cm plastic channels cut to length) were taken from Core JPC-13 from 527 cm to the base of the core for paleomagnetic studies and XRF scanning. Following these analyses, the u-channels were sampled by taking contiguous samples at 2.5-cm intervals. Each sample was dried, weighed, and washed over a 63-μm sieve. The sand fraction was dried and weighed to obtain the wt.% greater than 63 μm (wt.% >63 μm). The relative abundance of ice-rafted detritus was determined by splitting the >150 μm sediment fraction until approximately 300 lithic grains remained. IRD abundances are expressed as percent lithic fragments of total grains counted.

Stable isotopic measurements were made on planktonic (*Neogloboquadrina pachyderma* sinistral and *Globigerina bulloides*) and benthic (*Cibicidoides wuellerstorfi*) foraminifera. Specimens of *C. wuellerstorfi* were selected from the >150 μm size fraction, *N. pachyderma* (sinistral) from the 150 to 250 μm fraction, and *G. bulloides* from the 300 to 350 μm size fraction. Foraminifer tests were soaked in ~15% H_2O_2 for 30 min to remove organic matter, and were then rinsed with methanol and sonically cleaned to remove fine-grained particles. The methanol was removed with a syringe, and samples were dried in an oven at 50 °C for 24 h. The foraminifer calcite was loaded into individual reaction vessels, and each sample was reacted with three drops of H_3PO_4 (specific gravity = 1.92) using a ThermoFinnigan MAT Kiel III carbonate preparation device. Isotope ratios were measured online using a ThermoFinnigan MAT 252 mass spectrometer. Analytical precision was estimated to be ±0.08 for $\delta^{18}O$ and ±0.04‰ for $\delta^{13}C$ by measuring 8 standards (NBS-19, total = 291) with each set of 38 samples. For stable isotopic analysis of bulk carbonate we followed the method detailed by Hodell and Curtis (2008).

Anhysteretic susceptibility (k_{ARM}) divided by volume susceptibility (k) is a commonly used grain-size proxy for magnetite in both marine and lake sediments (King et al., 1983; Tauxe, 1993). For JPC-13, values of k_{ARM} and k were measured on the u-channel samples using a 2G Enterprises cryogenic magnetometer and a susceptibility track designed for u-channel samples (Thomas et al., 2003). Higher (lower) values of the k_{ARM}/k ratio correspond to lower (higher) mean magnetic (magnetite) grain size. The grain-size calibration of the k_{ARM}/k ratio, following King et al. (1983), indicates mean magnetite grain sizes below 10 μm for most pelagic sediments (including JPC-13). The k_{ARM}/k ratio may, however, be affected by magnetic grains in the sortable-silt (10–63 μm) fraction influenced by hydrodynamic bottom-current sorting.

High-resolution (2.5-mm) XRF core scanning measurements were obtained on u-channel subcores at the University of Cambridge using an Avaatech XRF core scanner (Richter et al., 2006). The core surface irradiated was 6-mm (cross-core) by 2.5 mm (downcore) with a count time of 40 s. Three scans were performed every 2.5 mm at 10, 30 and 50 kv and 0.2 mA to obtain both light and heavy elements. Results are presented as log ratios that provide a reliable signal of relative changes in chemical composition (Weltje and Tjallingii, 2008).

4. Chronology

Core JPC-13 extends from the Holocene (MIS 1) to the Last Interglacial (MIS 5e) (Fig. 2). For the interval from 0 to 80 ka, the time scale (SFCP04) was derived by correlating the benthic $\delta^{18}O$ record of JPC-13 to the benthic $\delta^{18}O$ record of core MD95-2042 from the Portuguese Margin (Shackleton et al., 2004). The millennial-scale features in benthic $\delta^{18}O$ are very similar between the two sites (Fig. 2) and also with IODP Site U1308 (Hodell et al., 2008). As noted by Shackleton et al. (2000, 2004), the benthic $\delta^{18}O$ signal at MD95-2042 (and JPC-13) resembles Antarctic temperature variability (e.g., warming events A1–A4). The chronology beyond 80 ka was derived by correlating benthic $\delta^{18}O$ to the LR04 stack of Lisiecki and Raymo (2005) and is shown for completeness (Fig. 2).

North Atlantic Ash Zones 1 (AZ1) and 2 (AZ2) are identified in JPC-13 providing two additional tie points for correlation to other

North Atlantic marine sediment and Greenland ice cores (Fig. 3). AZ1 is centered at 622 cm and is composed of several ashes that are widely dispersed across the North Atlantic including the Vedde Ash, which is dated at ~12.1 ka within the Younger Dryas Chronozone (Lacasse et al., 1995; Zielinski et al., 1997; Thornalley et al., 2010).

Ash Zone 2 (AZ2) occurs at 1151 cm and is dated at 53.26 ± 5% ka (Meese et al., 1994), coinciding with the rapid climate transition (cooling) at the end of Greenland Interstadial (GIS) 15 (Austin et al., 2004). The date of AZ2 in our record on the SFCP time scale is 55.7 ka.

A prominent low in relative paleointensity, associated with the Laschamp geomagnetic excursion, occurs at 907.5 cm in core JPC-13. In the North Atlantic, the Laschamp typically lies 20–30 cm beneath the IRD layer of Heinrich Event 4 (Thouveny et al., 2008). Our placement of Heinrich 4 at 884 cm is consistent with this observation. The Laschamp has been correlated to Greenland IS10 based on a peak in cosmogenic nuclide abundance and is dated at 40.4 ± ka (Guillou et al., 2004).

During the last glacial period, sedimentation rates average 20 cm kyr^{-1} but vary from as low as 7 cm kyr^{-1} to as high as 90 cm kyr^{-1}. Given a sampling interval of 2.5 cm, the average temporal resolution of the record is about 124 years. The SFCP04 chronology was used not because it is necessarily the most accurate or current time scale (Skinner, 2008), but rather because both marine and polar ice core records can be confidently placed on this time scale.

5. Results

5.1. Ice-rafted detritus

Ice-rafted detritus layers in JPC-13 are marked by peaks in percent lithic grains, wt.% coarse fraction, and increases in magnetic grain size (k_{ARM}/k) (Fig. 3). IRD consists dominantly of quartz and volcanic grains. Coarse lithic peaks occur at each of the Heinrich events although they lack the large amounts of coarse-grained detrital carbonate found in the IRD belt to the south (Fig. 1). Increases in fine-grained detrital carbonate are indicated by decreases in bulk carbonate $\delta^{18}O$ (Hodell and Curtis, 2008). IRD peaks are also associated with cold events C19, 20 and 21 identified by McManus et al. (1994). Two of the coarse lithic peaks coincide

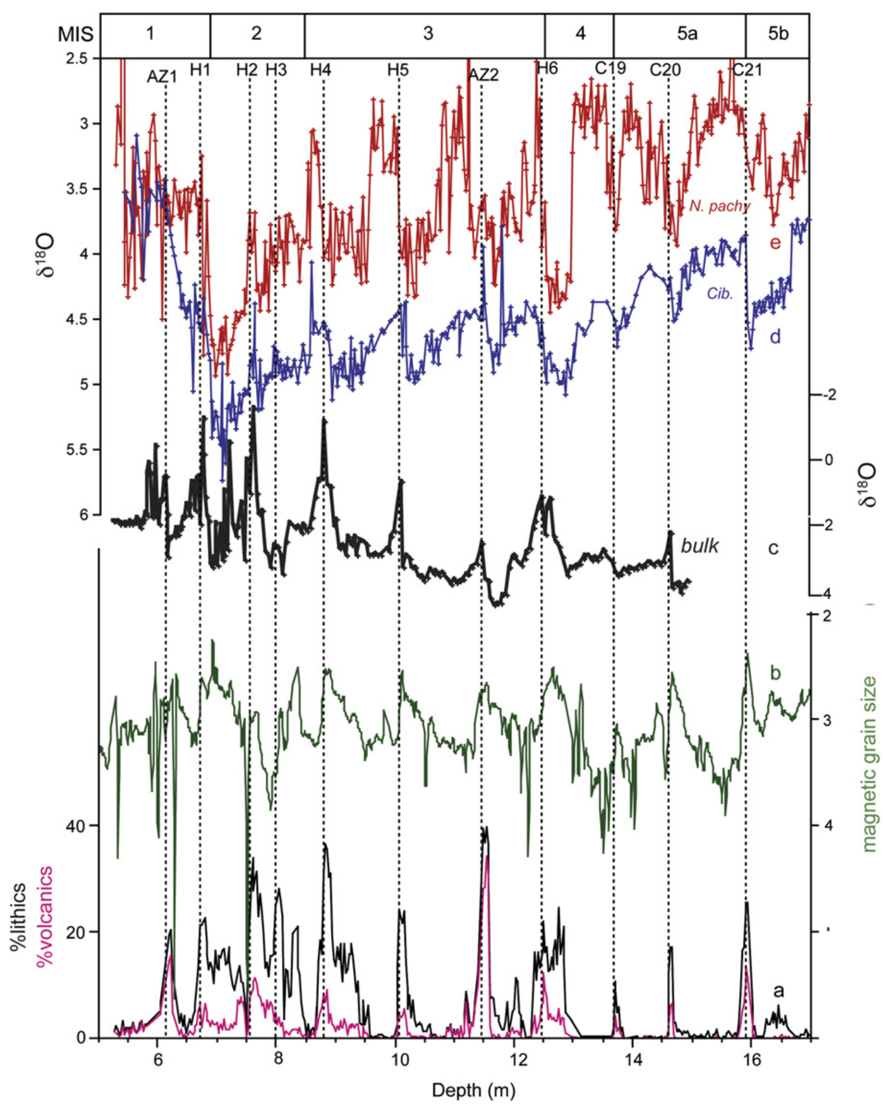

Fig. 3. Ice-rafted detritus proxies from Core JPC-13 including (a) percent total lithics (black) and volcanics (magenta), (b) magnetic grain size (k_{ARM}/k) (green) coarsening for lower values (upward), and (c) bulk carbonate $\delta^{18}O$ (gray). Also shown are $\delta^{18}O$ records of (d) *C. wuellerstorfi* (blue) and (e) *N. pachyderma* (red) from Core JPC-13. Vertical dashed lines mark the position of Heinrich (H) events, cold (C) periods of McManus et al. (1994), and Ash zones (AZ) 1 and 2. (For interpretation of the references to colour in this figure legend, the reader is referred to the web version of this article.)

with ash layers (AZ1 and 2) and are dominated by volcanic material (Fig. 3).

5.2. Stable isotopes

The benthic $\delta^{18}O$ of JPC-13 is marked by a series of millennial-scale oscillations of triangular form beginning with sharp decreases followed by more gradual increases (Fig. 4). The sharp benthic $\delta^{18}O$ decreases are labeled A1–A7 assuming these events are synchronous with warmings in the Antarctic ice cores as observed by Shackleton et al. (2000). Each of the benthic $\delta^{18}O$ decreases is associated with an increase in percent IRD and sediment coarse fraction. The benthic $\delta^{18}O$ variations during MIS 3 are on the order of 0.3–0.5‰. The transition from MIS 5a to 4 is marked by two millennial-scale decreases (labeled A5 and A6) superimposed upon a more gradual trend of increasing $\delta^{18}O$. The benthic $\delta^{18}O$ change from MIS 5b to 5a is abrupt as is the transition from MIS 5b to 5c and 5d to 5c with an amplitude of 0.6 and 0.4‰, respectively (Figs. 2 and 4). The 5e–5d part of the record is discussed by Hodell et al. (2009).

The $\delta^{18}O$ record of *N. pachyderma* has a "square-wave" form and shows a variable lag with respect to the benthic $\delta^{18}O$ signal for events A1–A7. The $\delta^{18}O$ of *G. bulloides* shows more millennial-scale structure than the $\delta^{18}O$ of *N. pachyderma.* Prominent decreases in the $\delta^{18}O$ of *G. bulloides* and *N. pachyderma* follow each of the IRD peaks (Fig. 4). This pattern of decreasing planktic $\delta^{18}O$ following IRD layers in JPC-13 differs from other North Atlantic records from the IRD belt to the south where low planktonic $\delta^{18}O$ coincides with Heinrich layers (Bond et al., 1993, 1997; Rashid and Boyle, 2007).

6. Discussion

6.1. IRD and surface water hydrography

Core JPC-13 is on the northern margin of the IRD belt (Robinson et al., 1995). The IRD in the core is composed principally of quartz and basaltic glass with ancillary volcanic and sedimentary rock fragments derived from multiple sources including Iceland, Europe, North America and Greenland (van Kreveld et al., 2000). Coarse-grained detrital carbonate is lacking but Hodell and Curtis (2008) proposed the $\delta^{18}O$ of bulk carbonate in North Atlantic sediments may be used to recognize sediment layers containing detrital carbonate, especially near the margins of the IRD belt where fine-fraction detrital carbonate may be transported. Andrews (2000) pointed out that the greatest proportion of ice-rafted sediment is in the clay and silt fractions. It is this fine fraction that is more likely to be transported greater distances by currents and eddies than is coarse-grained IRD.

Because the $\delta^{18}O$ of detrital carbonate from Hudson Strait averages −5.5‰ compared to biogenic carbonate of +4 to +5‰, bulk $\delta^{18}O$ decreases when detrital carbonate is present (Fig. 5) (Hodell and Curtis, 2008). Each of the peaks in % lithics in Core JPC-13 is associated with a decrease in bulk carbonate $\delta^{18}O$, suggesting they are correlative with Heinrich layers in the IRD belt to the south (Fig. 6). Heinrich Layers 1, 2, 4 and 5 have the lowest bulk $\delta^{18}O$ consistent with a Hudson Strait source for these events (Hemming, 2004). We attribute these low bulk $\delta^{18}O$ values to the occurrence of fine-grained detrial carbonate transported from the IRD belt and of Laurentide origin, although we cannot entirely eliminate additional carbonate sources from Europe or older reworked marine sediment. Each of the lithic peaks, including the Heinrich Events, shows a concomitant increase in volcanic material derived from Iceland (Fig. 3) (Lacasse et al., 1998) or possibly East Greenland (Andrews et al., 1999). Volcanic grains have been found to be associated with Heinrich events in the IRD belt to the south and precede slightly the occurrence of detrital carbonate (Bond and Lotti, 1995).

IRD peaks in JPC-13 do not coincide with low planktonic $\delta^{18}O$ as they do in the central IRD belt to the south, suggesting they were not associated with abundant meltwater. Instead, low planktonic $\delta^{18}O$ immediately follows the IRD peaks (Fig. 4). The pronounced decreases in $\delta^{18}O$ of *N. pachyderma* and *G. bulloides* following the benthic $\delta^{18}O$ decrease and IRD peaks could represent either warmer temperatures and/or reduced surface salinity. The absence of IRD during the $\delta^{18}O$ minima argues against iceberg melting unless the ice bergs were clean (i.e., devoid of detritus) or melted elsewhere and the low-$\delta^{18}O$ water was transported to the site (Elliot et al., 1998). The lack of a planktonic $\delta^{18}O$ decrease associated with Heinrich events in JPC-13 is consistent with results of Cortijo et al. (2000) who found no significant changes in salinity during H4 north of 51°N in contrast to cores from the IRD belt to the south

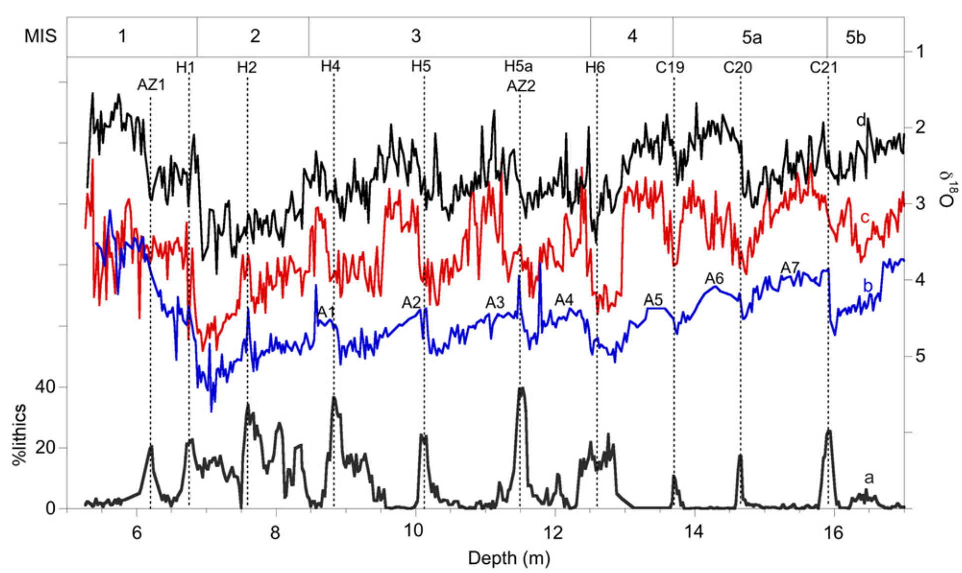

Fig. 4. (a) Percent lithics (black) and $\delta^{18}O$ records of (b) *Cibicidoides* (blue), (c) left-coiling *N. pachyderma* (red) and (d) *G. bulloides* (black). Also shown are position of Heinrich (H) and cold (C) events (McManus et al., 1994), Antarctic warm events (A1–A7), Ash zones (AZ) 1 and 2, and Marine Isotope Stages (MIS). Dashed vertical lines designate lithic peaks that coincide with decreases in benthic $\delta^{18}O$. (For interpretation of the references to colour in this figure legend, the reader is referred to the web version of this article.)

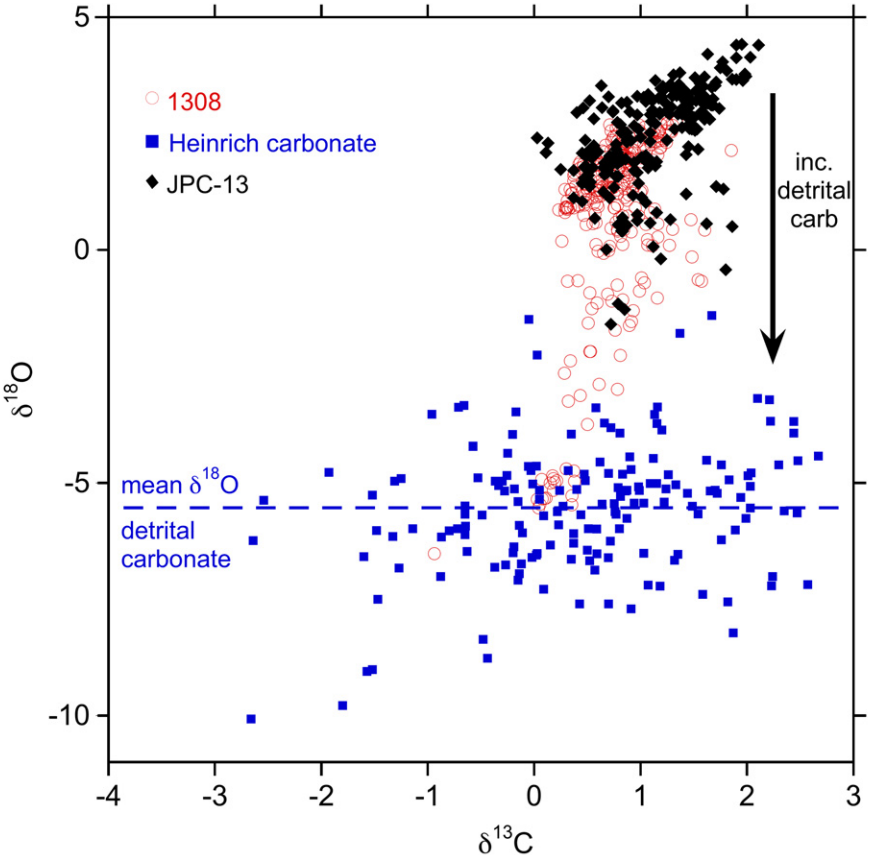

Fig. 5. $\delta^{18}O$ and $\delta^{13}C$ of bulk carbonate in Core JPC-13 (black diamonds) and Site U1308 (red circles) compared with values from individual detrital carbonate grains (blue squares) from Heinrich layers (Hodell and Curtis, 2008). (For interpretation of the references to colour in this figure legend, the reader is referred to the web version of this article).

between 40 and 50°N. It is also possible that the low planktonic $\delta^{18}O$ values reported during Heinrich events in the IRD belt have been over estimated because of the incomplete removal of detrital carbonate from the internal chambers of foraminifer tests (Hodell and Curtis, 2008).

Elliot et al. (1998) observed a similar phase relationship between IRD and planktonic $\delta^{18}O$ in the Irminger Basin where low planktonic $\delta^{18}O$ occurred a few 100 years after the peak in IRD. They interpreted this lag as reflecting low-salinity water derived from northward propagation of iceberg meltwater produced in the IRD belt to the south. We instead attribute the low planktonic $\delta^{18}O$ events to the abrupt warmings that immediately followed Heinrich stadials and coincided with the longest, warmest interstadials in Greenland. This interpretation is supported by the warm sea

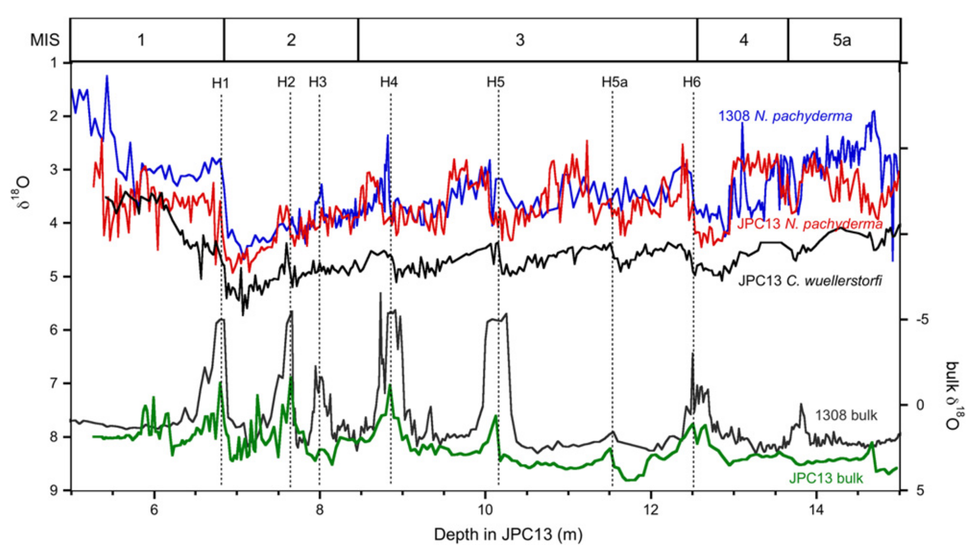

Fig. 6. (bottom) Comparison of bulk carbonate (gray) and *N. pachyderma* $\delta^{18}O$ (green) for IODP Site U1308 and JPC-13. Correlation was derived by matching minima in bulk carbonate $\delta^{18}O$ that mark Heinrich layers. (top) Oxygen isotope records of foraminifera including *C. wuellerstorfi* (black) from Core JPC-13 and *N. pachyderma* from Site U1308 (blue) and JPC-13 (red). (For interpretation of the references to colour in this figure legend, the reader is referred to the web version of this article.)

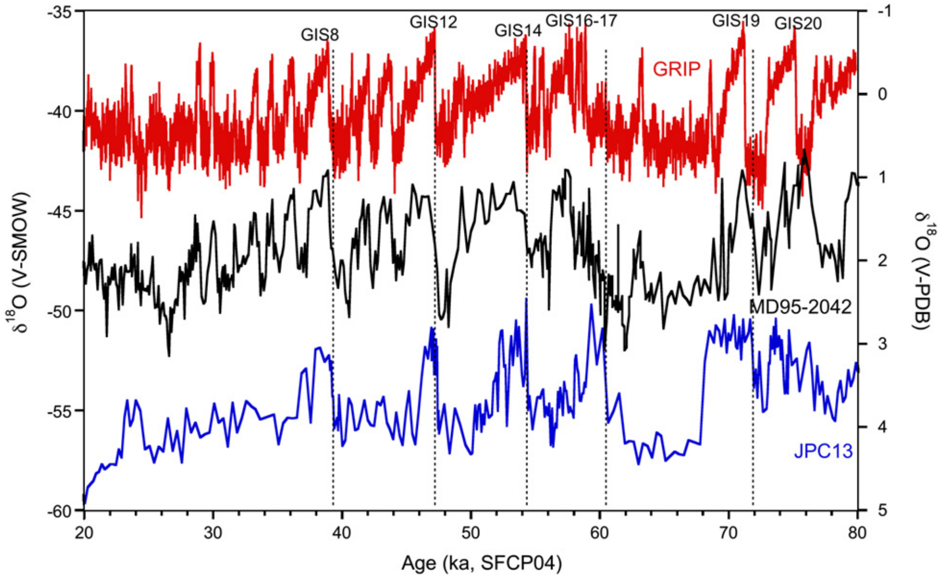

Fig. 7. Comparison of $\delta^{18}O$ of *N. pachyderma* from JPC-13 (blue), *G. bulloides* from Core MD95-2042 (black), and GRIP ice core (red) from 20 to 80 ka. Both records are on the SFCP04 time scale. (For interpretation of the references to colour in this figure legend, the reader is referred to the web version of this article.)

surface temperatures that immediately follow IRD in other cores from the Reykjanes Ridge at 59°N (van Kreveld et al., 2000; Jonkers et al., 2010a). Using the SFCP04 time scale, each of the lows in *N. pachyderma* $\delta^{18}O$ in Core JPC-13 correlates with a similar magnitude decrease in planktonic $\delta^{18}O$ in Iberian Margin Core MD95-2042 and with long Greenland interstadials (Fig. 7). The low planktonic $\delta^{18}O$ at JPC-13 also correlates to those at Site U1308 (redrill of DSDP Site 609) in the IRD belt to the south (Fig. 6) (Hodell and Curtis, 2008).

The $\delta^{18}O$ of *N. pachyderma* following Heinrich events decreases by ~1‰ during MIS3 (Fig. 8). If attributed all to temperature, this would suggest ~4 °C of warming just below the base of the seasonal mixed layer where *N. pachyderma* (sin) calcifies (Jonkers et al., 2010a, b). Warm winter temperatures are also supported by foraminiferal transfer functions (van Kreveld et al., 2000) and $\delta^{15}N$ of gas from Greenland ice cores that typically indicate a rapid warming of ~12 °C at the start of the long interstadials following Heinrich events (Huber et al., 2006).

In cores at 59°N on the Reykjanes Ridge, Jonkers et al. (2010a) found that warming of surface water began earlier during the time of IRD deposition and preceded the main warming associated with the pronounced interstadial following the Heinrich event (see also Moros et al., 2002). They attributed the warm temperatures

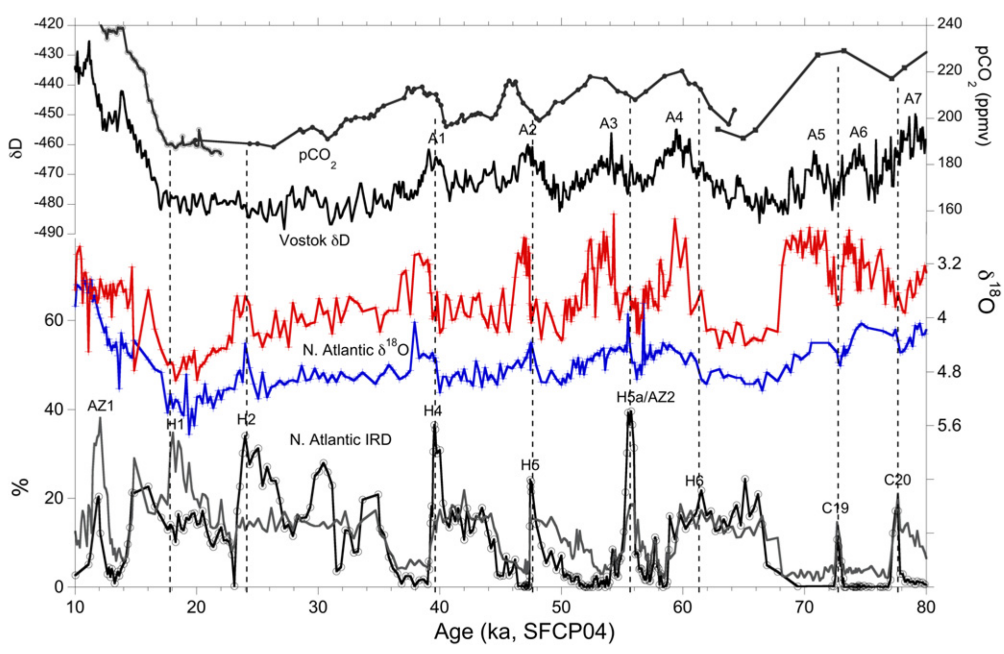

Fig. 8. Percent lithics (black open circles), wt.% >63 μm fraction (gray), and $\delta^{18}O$ records of *Cibicidoides* (blue crosses), left-coiling *N. pachyderma* (red crosses), δD of the Vostok ice core (black line), and *p*CO_2 composite from Antarctic ice cores (open circles from Byrd, filled circles from Taylor Dome, filled squares from Vostok). Dashed vertical lines designate lithic peaks including Heinrich events, C-events and Ash Zones 1 and 2. All records on SFCP04 time scale expect CO_2 which is on EDC-3. (For interpretation of the references to colour in this figure legend, the reader is referred to the web version of this article.)

during IRD events at ~59°N to the presence of a subsurface warm layer that seasonally shoaled during summer. We do not observe decreasing $\delta^{18}O$ of *N. pachyderma* or *G. bulloides* during IRD deposition at 53°S, but our $\delta^{18}O$ results strongly support the temperature maxima that occurred after IRD deposition ceased (van Kreveld et al., 2000; Jonkers et al., 2010a). Mg/Ca and faunal abundance counts of foraminifera are needed in Core JPC-13 to determine if seasonal warming during IRD deposition may have preceded the main planktonic $\delta^{18}O$ decrease.

6.2. Phasing of isotopic and IRD proxies

The relative phasing of variables can be observed in the depth domain and is independent of the age model applied (Fig. 8). We find a similar phasing in surface and deep-water $\delta^{18}O$ as reported by Shackleton et al. (2000); that is, benthic $\delta^{18}O$ leads planktonic $\delta^{18}O$ (Figs. 4 and 8). Each of the peaks in % lithics coincides with a decrease in benthic $\delta^{18}O$ followed by a decrease in the $\delta^{18}O$ of *Neogloboquadrina pachyderma* and *G. bulloides* (Figs. 6 and 8). This phasing supports previous results indicating the coldest stadials in Greenland (e.g., Heinrich stadials) occurred during times of warming in Antarctica with the onset of GIS events 8, 12, 14, 16/17, 19, 20, and 21 by 1.5–3 kyr (Blunier and Brook, 2001; Capron et al., 2009).

Although determining the phase relationships in a single core avoids some of the problems associated with time scale inaccuracy, it is not without other complications related to changes in sedimentation rate, sampling resolution, and bioturbation that can affect the nature and timing of paleoenvironmental signals. For example, lower sedimentation rates will attenuate the signal and obscure phasing among variables. Mean sedimentation rates are high in Core JPC-13, averaging 20 cm kyr^{-1}, but interval rates vary from as low as 7 cm kyr^{-1} to as high as 90 cm kyr^{-1}.

The *N. pachyderma* $\delta^{18}O$ records the warmest interstadials in the Greenland ice core (GIS8, 12, 14, 16–17) immediately following the Heinrich events (Bond et al., 1993), but the shorter, intervening interstadials are less well defined. This pattern may reflect the greater attenuation of signal for the shorter-term Dansgaard–Oeschger (D–O) events than for the longer-duration interstadials. For example, GIS 8, 12 and 14 and 16–17 were nearly twice as long as the other interstadials.

Anderson (2001) estimated a 70% reduction in amplitude of short-term D–O events for sedimentation rates of 10 cm kyr^{-1}. For longer-duration events, sedimentation rates of 10 cm kyr^{-1} preserve 50% of the original signal, whereas 95% of the original signal is captured at 50 cm kyr^{-1} (Anderson, 2001).

During times of rapid change, such as Heinrich stadials followed by abrupt warming, phase shifts can be induced for species with opposite abundance patterns (Hutson, 1980; Löwenmark and Grootes, 2004; Löwemark et al., 2008). For example, the $\delta^{18}O$ decrease following Heinrich events at JPC-13 occurs earlier in *G. bulloides* than *N. pachyderma* (sin) (Fig. 4). *N. pachyderma* (sin) was more abundant during the Heinrich stadials in the subpolar North Atlantic, whereas *G. bulloides* was more prevalent during Greenland interstadials (Van Kreveld et al., 2000). Bioturbation will tend to move particles from levels of higher to lower concentration thereby resulting in a mixing down of isotopically lighter specimens of *G. bulloides* into the underlying IRD layer and mixing up of stadial *N. pachyderma* specimens into the interstadial. Bioturbation coupled with changing species abundance can explain the apparent lead in *G. bulloides* $\delta^{18}O$ relative to *N. pachyderma* (sin) (Fig. 4).

It is difficult to evaluate how changes in the relative abundance of benthic foraminifer taxa might influence phasing because their abundance and species composition are not only affected by physio-chemical properties of water masses but also by organic carbon rain from the surface. It is unlikely the benthic lead over planktonic $\delta^{18}O$ is an artefact of bioturbation and changing species abundance in MD95-2042 or JPC-13 because the phasing is independently supported by methane synchronization of polar ice cores (Blunier and Brook, 2001; EPICA Community Members, 2006).

Establishment of the phase relationships for the last glacial period in Core JPC-13 is important because it paves the way for applying similar methods to study phase relationships in older glacial periods of the Pleistocene at IODP Site U1304 drilled at the same location. The Site U1304 record extends to the top of the Olduvai Subchronozone (1.77 Ma) (Expedition 303 Scientists, 2006).

6.3. A pervasive Antarctic-type signal in the North Atlantic?

Pisias et al. (2010) demonstrated two leading modes of low-frequency global climate variability during MIS 3: a Greenland or “northern” mode and an Antarctic or “southern” mode (see also Clark et al., 2007). To the extent that benthic $\delta^{18}O$ reflects an Antarctic signal, IRD peaks in the North Atlantic also display a distinct Antarctic-type pattern. We suggest that the $\delta^{18}O$ of *N. pachyderma* also shows an Antarctic-style pattern, albeit with a time delay with only the largest and longest interstadials following Antarctic warming events clearly expressed in the planktonic $\delta^{18}O$ record of the subpolar North Atlantic (Fig. 8).

Barker and Knorr (2007) similarly suggested that Antarctic-style climate variability is a globally pervasive pattern that is even embedded in Greenland ice cores. Increases in atmospheric CO_2 accompanied the millennial-scale warming events in Antarctica during MIS 3, thereby providing a mechanism for global propagation of the Antarctic climate signal (Fig. 8) (Indermühle et al., 2000; Ahn and Brook, 2008).

The Antarctic signal is prevalent in subpolar surface waters but is delayed because iceberg melting and sea-ice expansion during Heinrich events kept the subpolar North Atlantic cold despite warming elsewhere (Moros et al., 2002). Because the low-salinity surface layer was underlain by a warm subsurface water (Mignot et al., 2007), abrupt warming ensued once the rate of iceberg calving diminished and surface stratification broke down. Schmittner et al. (2002) used an Earth System Climate Model to show that reduced iceberg calving following Heinrich events can act as a trigger for rapid warming within several 100 years. Jonkers et al. (2010a) similarly suggested that the abrupt warming following Heinrich events was related to the rapid emptying of a subsurface heat reservoir that restarted overturning circulation.

6.4. Northward heat transport and deep-water circulation

A change in the strength of AMOC is commonly invoked to explain anti-phasing of millennial-scale climate variability between Greenland and Antarctica (Broecker, 1998; Alley, 2007) although sea-ice and tropical processes may also play important roles (Clement and Peterson, 2008). AMOC was reduced during Heinrich events as lowered sea surface salinity decreased overturning and permitted the southern expansion of sea ice in the North Atlantic. This process is expressed in benthic $\delta^{13}C$ variations in Core MD95-2042 that show lower values during stadials and higher values during interstadials (Fig. 9) (Skinner et al., 2007; Martrat et al., 2007). The IRD peaks (Heinrich events) in JPC-13 coincide with benthic $\delta^{13}C$ minima in MD95-2042 indicating a link between surface-deep North Atlantic hydrography (Fig. 9). Benthic $\delta^{13}C$ in Core JPC-13 also decreases across H1, H2, H4 and H5 although the pattern is not as clear as MD95-2042 (Fig. 10).

Several lines of evidence in JPC-13 suggest that ISOW was stronger during the warmer, longer Greenland interstadials (e.g., GIS

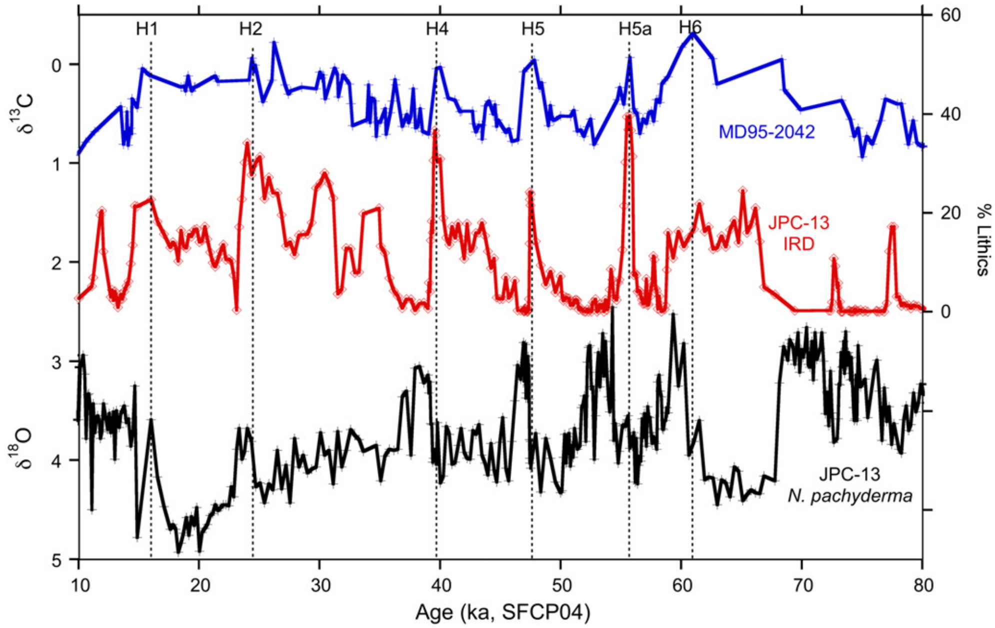

Fig. 9. Benthic $\delta^{13}C$ of Core MD95-2042 Shackleton et al. (2004) (blue) compared with percent lithics (red) and $\delta^{18}O$ of *N. pachyderma* (black) from Core JPC-13. The IRD peaks in JPC-13 are generally associated with lows in benthic $\delta^{13}C$ (note scale decreases in upwards direction). (For interpretation of the references to colour in this figure legend, the reader is referred to the web version of this article.)

8, 12, and 14) that immediately followed Heinrich events. Abrupt warming in Greenland following Heinrich events coincided with increases in benthic $\delta^{13}C$ in Core MD95-2042 and decreases in sediment grain size in Core JPC-13 (Fig. 11). During each of the long Greenland interstadials, sediments are dominated by silt and clay and the wt.% coarse fraction is low in Core JPC-13. The sand fraction (>63 μm) on the southern Gardar Drift consists of foraminifera and IRD, and is strongly diluted by silt and clay transported by ISOW (Bianchi and McCave, 2000). We suggest the decreases in grain size during MIS 3 are the result of increased transport of fine sediment by ISOW associated with the longest, warmest Greenland interstadials (GIS 8, 12,14, 16–17). Magnetic grain size (k_{ARM}/k) also decreases at these times suggesting increased transport of fine-grained magnetite by ISOW to the southern end of the Gardar Drift (Fig. 3). We do not believe that k_{ARM}/k reflects current speed as grains contributing this parameter are probably too small to be hydrodynamically sorted. The parameter probably primarily denotes changes in the contribution of fine grained detritus from northern (Icelandic) sources (see Kissel et al., 2009).

Further support for changes in ISOW is provided by K/Ti ratios that reflect the relative contribution of acid (felsic) and basic (mafic) sources of terrigenous sediment (Prins et al., 2001; Richter et al., 2006; Ballini et al., 2006; Grützner and Higgins, in press). Low K/Ti in Core JPC-13 occurred during the Holocene and MIS 5 when ISOW was strong and transported fine-grained sediment south from the Iceland basaltic province (Fig. 11), thereby building the Gardar Drift. K/Ti in Core JPC-13 was also relatively low during each of the long, warm interstadials of MIS 3 when increasing benthic

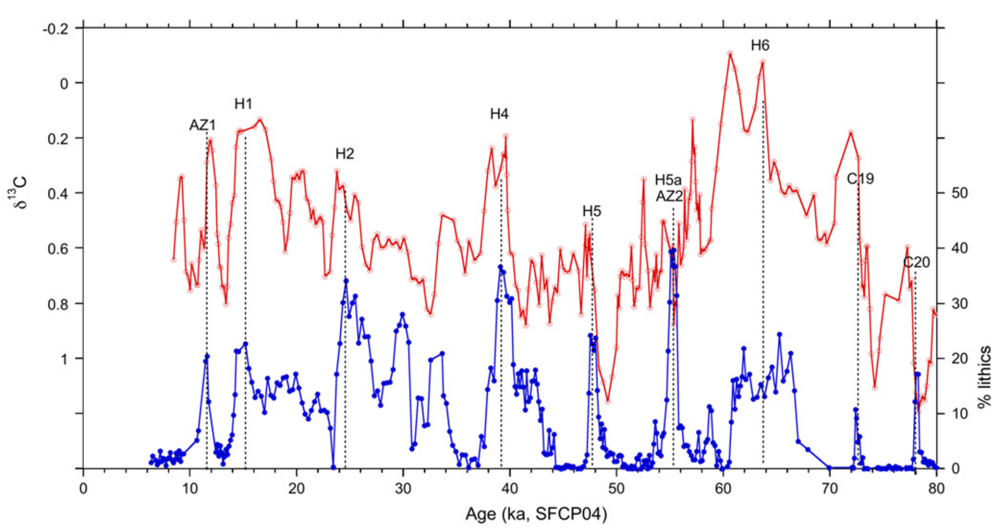

Fig. 10. Benthic $\delta^{13}C$ (red; 3-pt running average) and % lithics (blue) in Core JPC-13. (For interpretation of the references to colour in this figure legend, the reader is referred to the web version of this article.)

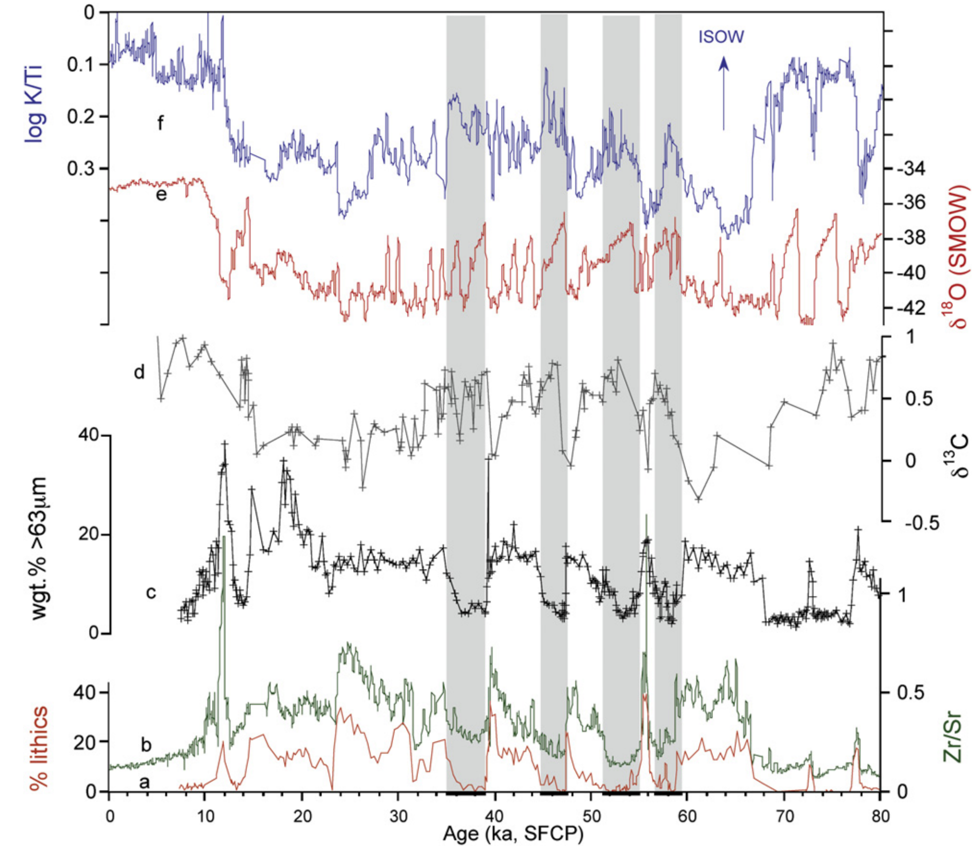

Fig. 11. (a) % lithics and (b) Sr/Zr (and IRD proxy) and (c) wt.% >63 μm sediment coarse fraction in Core JPC-13 (d) benthic $\delta^{13}C$ in Core MD95-2042; (e) Greenland ice core $\delta^{18}O$; and (f) log*K*/Ti in Core JPC-13. (For interpretation of the references to colour in this figure legend, the reader is referred to the web version of this article.)

$\delta^{13}C$ and decreasing grain size also support increased convection in the Nordic Seas (Fig. 11).

Results from Core JPC-13 support previous findings for increased heat transport to the high latitudes, northward penetration of the North Atlantic Current, and increased meridional overturning during the warmest, longest Greenland interstadials of MIS 3 (Piotrowski et al., 2008; Kissel et al., 2008). Strong northward heat transport and warming of the subpolar North Atlantic and Greenland following Antarctic warm events may have been related to the abrupt resumption of AMOC following Heinrich events (Schmittner et al., 2002; Knorr and Lohmann, 2007; Liu et al., 2009).

6.5. *Benthic $\delta^{18}O$, ice volume, and deep hydrographic change*

Results from Core JPC-13 confirm that decreases in benthic $\delta^{18}O$ coincided with peaks in IRD during the last glaciation on the southern Gardar Drift, and were correlated with warmings events in Antarctica (A1–A7). The Antarctic-like, millennial-scale variations in benthic $\delta^{18}O$ appear to be a robust feature of North Atlantic records at water depths between 3 and 4 km (Fig. 2). Although independent studies indicate that climate variability in the high-latitude North Atlantic and Antarctica were tightly coupled during the last glaciation (e.g., EPICA Community Members, 2006), it is not entirely clear why the benthic $\delta^{18}O$ signal in the North Atlantic has the same character and phasing as Antarctic ice cores.

Changes in the $\delta^{18}O$ of benthic foraminifera reflect a combination of temperature, global ice volume (sea level), and local hydrographic effects (Waelbroeck et al., 2002; Skinner et al., 2003). There is considerable uncertainty, however, over the relative importance of these processes. Shackleton et al. (2000) originally interpreted the millennial changes in benthic $\delta^{18}O$ during MIS 3 on the Iberian Margin as indicating significant variations in ice volume.

The benthic $\delta^{18}O$ variations at JPC-13 are on the order of 0.3–0.5‰ for A1–A4, which would permit up to 30–50 m of sea-level variation if all the change was attributed to ice volume. Sea-level rise during the warm events in Antarctica is supported by the Red Sea $\delta^{18}O$ record, which indicates rather large sea-level variations that are similar to Antarctic-style climate variations (Siddall et al., 2003, 2008; Rohling et al., 2004, 2008) proposed at least four millennial-scale sea-level fluctuations of 20–30 m magnitude during MIS 3 with rises occurring during warming events in Antarctica and cold stadial conditions in Greenland (see also Gonzalez and Dupont, 2009). Sea-level rise during the Antarctic warm events may have been related to both dynamic and steric effects that, in turn, may have triggered a dynamic response of the Laurentide Ice Sheet (e.g., Flückiger et al., 2006). However, other studies have suggested that sea-level highstands coincided with Greenland interstadials and post-dated Antarctic warming (Arz et al., 2007; Sierro et al., 2009).

Skinner et al. (2003, 2007) demonstrated that only part of the benthic $\delta^{18}O$ signal in MIS 3 could be related to changes in continental ice volume with the remainder attributed to temperature and hydrographic change. Skinner and Elderfield (2007) found abrupt warming of deep-water during the middle of Heinrich stadials 4 and 5 indicating important changes in deep-sea temperature distribution. A subsurface heat reservoir at depth in the North Atlantic may have contributed to the rapid warming that followed

Heinrich events once breakdown of surface stratification occurred (Schmittner et al., 2002; Shaffer et al., 2004; Mignot et al., 2007).

This study demonstrates that each of the benthic $\delta^{18}O$ decreases in JPC-13 coincides with a peak in IRD, suggesting a possible link with ice bergs and/or sea ice (Fig. 4). Van Kreveld et al. (2000) proposed that decreasing benthic $\delta^{18}O$ in the Irminger Sea, which occurred just prior to the abrupt warmings in Greenland, may be related to a brine water pulse induced by seasonal freezing of large parts of the northwestern Atlantic during Heinrich events. Hillaire-Marcel and de Vernal (2008) similarly proposed that light isotopic excursions in *N. pachyderma* associated with Heinrich events could be related to episodes of enhanced sea-ice formation. The mixing of cold, low-$\delta^{18}O$ brine water and poorly ventilated deep-water from the Southern Ocean during Heinrich events might explain the occurrence of a cold, low-$\delta^{18}O$ and low-$\delta^{13}C$ water mass during Heinrich stadials (Skinner et al., 2007). Explaining why the benthic $\delta^{18}O$ signal so closely follows an Antarctic-style pattern remains an important problem for understanding mechanisms of interhemispheric climate change.

7. Conclusions

Results from Core JPC-13 demonstrate that decreases in benthic $\delta^{18}O$ coincided with peaks in IRD during the last glaciation on the southern Gardar Drift. The IRD events are correlated with warming events in Antarctica (A1–A7), supporting a coupling of climate variability between the high-latitude North Atlantic and Antarctica during the last glaciation. The Antarctic warmings correspond to the coldest stadials in Greenland, associated with Heinrich events at the end of Bond cycles. The IRD pulses are followed shortly thereafter by abrupt decreases in planktonic $\delta^{18}O$ indicating warming of SST that is correlated with the most pronounced interstadials in Greenland. These changes coincided with an increased strength of AMOC and associated heat transport to the subpolar North Atlantic. The observed phasing in Core JPC-13 is the same as that inferred from marine sediment cores on the Portuguese Margin (Shackleton et al., 2000) and polar ice cores synchronized using variations in atmospheric methane (Blunier and Brook, 2001). The method applied here can be extended to IODP Site U1304, at the same location as Core JPC-13, to study phase relationships during older glacial periods of the Pleistocene.

Acknowledgments

We thank Gianna Browne for technical assistance and Jim Wright and Greg Mountain for collecting Core KN166-14-13JPC and providing samples. We thank Peter Clark and an anonymous referee whose thoughtful reviews significantly improved the quality of the manuscript. This research was supported by NERC grant NE/H009930/1.

References

Ahn, J., Brook, E.J., 2008. Atmospheric CO_2 and climate on millennial time scales during the last glacial period. Science 322, 83–85.

Alley, R.B., 2007. Wally was right: predictive ability of the North Atlantic “conveyor belt” hypothesis for abrupt climate change. Annu. Rev. Earth Planet. Sci. 35, 241–272.

Anderson, D.A., 2001. Attenuation of millennial-scale events by bioturbation in marine sediments. Paleoceanography 16, 352–357.

Andrews, J.T., 2000. Icebergs and iceberg rafted detritus (IRD) in the North Atlantic: facts and assumptions. Oceanography 13, 100–108.

Andrews, J.T., Barber, D.C., Jennings, A.E., 1999. Errors in generating time-series and in dating events at late Quaternary millennial (radiocarbon) time-scales: examples from Baffin Bay, NW Labrador Sea, and East Greenland. Mechanisms of global climate change at millennial time scales. Geophys. Monogr. 112, 23–34.

Arz, H.W., Lamy, F., Ganopolski, A., Nowaczyk, N., Patzold, J., 2007. Dominant northern hemisphere climate control over millennial-scale glacial sea-level variability. Quaternary Sci. Rev. 26, 312–321.

Austin, W.E.N., Wilson, L.J., Hunt, J.B., 2004. The age and chronostratigraphical significance of north Atlantic ash zone II. J. Quat. Sci. 19 (2), 137–146.

Ballini, M., Kissel, C., Colin, C., Richter, T., 2006. Deep-water mass source and dynamic associated with rapid climatic variations during the last glacial stage in the North Atlantic: a multiproxy investigation of the detrital fraction of deep-sea sediments. Geochem. Geophys. Geosyst. 7 (Q02N01). doi:10.1029/2005GC001070.

Barker, S., Knorr, G., 2007. Antarctic climate signature in the Greenland ice core record. Proc. Nat. Acad. Sci. U.S.A. 104, 17278–17282.

Bianchi, G.G., McCave, I.N., 2000. Hydrography and sedimentation under the deep western boundary current on Björn and Gardar Drifts, Iceland Basin. Mar. Geol. 165, 137–169.

Blunier, T., Brook, E.J., 2001. Timing of millennial-scale climate change in Antarctica and Greenland during the last glacial period. Science 291, 109–112.

Blunier, T., Chappellaz, J., Schwander, J., Dallenbach, A., Stauffer, B., Stocker, T.F., Raynaud, D., Jouzel, J., Clausen, H.B., Hammer, C.U., Johnsen, S.J., 1998. Asynchrony of Antarctic and Greenland climate change during the last glacial period. Nature 394, 739–743.

Bond, G.C., Lotti, R., 1995. Iceberg discharges into the North Atlantic on millennial time scales during the last glaciation. Science 267, 1005–1010.

Bond, G., Showers, W., Cheseby, M., Lotti, R., Almasi, P., deMenocal, P., Priore, P., Cullen, H., Hajdas, I., Bonani, G., 1997. A pervasive millennial-scale cycle in North Atlantic Holocene and glacial climates. Science 278, 1257–1266.

Bond, G., Broecker, W., Johnsen, S., McManus, J., Labeyrie, L., Jouzel, J., Bonani, G., 1993. Correlations between climate records from North Atlantic sediments and Greenland ice. Nature 365, 143–147.

Broecker, W.S., 1998. Paleocean circulation during the last deglaciation: a bipolar seesaw? Paleoceanography 13 (2), 119–121.

Capron, E., Landais, A., Lemieux-Dudon, B., Schilt, A., Masson-Demotte, V., Buiron, D., Chappelaz, J., Dahl-Jensen, D., Johnsen, S., Leuenberger, M., Loulergue, L., Oerter, H., Chappelas, J., 2009. Synchronising EDML and NorthGRIP ice cores using $\delta^{18}O$ of atmospheric oxygen ($\delta^{18}Oatm$) and CH_4 measurements over MIS5 (80–123 kyr). Quaternary Sci. Rev.. doi:10.1016/j.quascirev.2009.07.014.

Charles, C.D., Lynch-Stieglitz, J., Ninnemann, U.S., Fairbanks, R.G., 1996. Climate connections between the hemisphere revealed by deep sea sediment core/ice core correlations. Earth Planet. Sci. Lett. 142, 19–27.

Clark, P.U., Hostetler, S.W., Pisias, N.G., Schmittner, A., Meissner, K.J., 2007. Mechanisms for a ~7-kyr climate and sea-level oscillation during marine isotope stage 3. In: Schmittner, A., Chiang, J., Hemming, S. (Eds.), Ocean Circulation: Mechanisms and Impacts. Geophysical Monograph, vol. 173. American Geophysical Union, Washington, D.C, pp. 209–246.

Clement, A.C., Peterson, L.C., 2008. Mechanisms of abrupt climate change of the last glacial period. Rev. Geophys. 46 (RG4002), 1–39.

Cortijo, E., Labeyrie, L., Vidal, L., Vautravers, M., Chapman, M., Duplessy, J.-C., Elliot, M., Arnold, M., Turon, J.-L., Auffret, G., 2000. Rapid climatic variability of the North Atlantic Ocean and global climate: a focus of the IMAGES program. Quaternary Sci. Rev. 19, 227–241.

Crowley, T.J., 1992. North Atlantic deep water cools the southern hemisphere. Paleoceanography 7, 489–497.

Elliot, M., Labeyrie, L., Bond, G., Cortijo, E., Turon, J.-L., Tisnerat, N., Duplessy, J.-C., 1998. Millennial-scale iceberg discharges in the Irminger Basin during the last glacial period: relationship with the Heinrich events and environmental settings. Paleoceanography 13 (5), 433–446.

EPICA Community Members, 2006. One-to-one coupling of glacial climate variability in Greenland and Antarctica. Nature 444, 195–198.

Expedition 303 Scientists, 2006. Site U1304. In: Channell, J.E.T., Kanamatsu, T., Sato, T., Stein, R., Alvarez Zarikian, C.A., Malone, M.J., Expedition 303/306 Scientists (Eds.), Proc. IODP, 303/306. Integrated Ocean Drilling Program Management International, Inc., College Station TX. doi:10.2204/iodp.proc.303306.104.2006.

Flückiger, J., Knutti, R., White, J.W.C., 2006. Oceanic processes as potential trigger and amplifying mechanisms for Heinrich events. Paleoceanography 21 (PA2014). doi:10.1029/2005PA001204.

Guillou, H., Singer, B.S., Laj, C., Kissel, C., Scaillet, S., Jicha, B.R., 2004. On the age of the Laschamp geomagnetic excursion. Earth Planet. Sci. Lett. 227, 331–343.

Gonzalez, C., Dupont, L.M., 2009. Tropical salt marsh succession as sea-level indicator during Heinrich events. Quaternary Sci. Rev. 28, 939–946.

Grützner, J., Higgins, S.M. Threshold behavior of millennial scale variability in deep water hydrography inferred from a 1.1 Ma long record of sediment provenance at the southern Gardar Drift. Paleoceanography, in press.

Heinrich, H., 1988. Origin and consequences of cyclic ice rafting in the northeast Atlantic Ocean during the past 130,000 years. Quaternary Res. 29, 142–152.

Hemming, S.R., 2004. Heinrich events: massive late Pleistocene detritus layers of the North Atlantic and their global climate imprint. Rev. Geophys. 42 (RG1005). doi:10.1029/2003RG000128.

Hillaire-Marcel, C., de Vernal, A., 2008. Stable isotope clue to episodic sea ice formation in the glacial North Atlantic. Earth Planet. Sci. Lett. 268, 143–150.

Hodell, D.A., Curtis, J.H., 2008. Oxygen and carbon isotopes of detrital carbonate in North Atlantic Heinrich Events. Mar. Geol. 256, 30–35.

Hodell, D.A., Minth, E.K., Curtis, J.H., Hall, I.R., Channell, J.E.T., Xuan, C., 2009. Surface and deep water hydrography on Gardar drift (Iceland Basin) during the Last Interglacial period. Earth Planet. Sci. Lett. 288, 10–19.

Hodell, D.A., Channell, J.E.T., Curtis, J., Romero, O., Röhl, U., 2008. Onset of "Hudson Strait" Heinrich events in the eastern north Atlantic at the end of the middle Pleistocene transition ($\sim$640 ka)? Paleoceanography 23. doi:10.1029/2008PA001591.

Huber, C., Leuenberger, M., Spahni, R., FlückigerSchwander, J., Stocker, T.F., Johnsen, S., Landais, A., Jouzel, J., 2006. Isotope calibrated Greenland temperature record over Marine isotope stage 3 and its relation to CH_4. Earth Planet. Sci. Lett. 243, 504–519.

Hutson, W.M., 1980. Bioturbation of deep-sea sediments: oxygen isotopes and stratigraphic uncertainty. Geology 8, 127–130.

Indermühle, A., Monnin, E., Stauffer, B., Stocker, T.F., Wahlen, M., 2000. Atmospheric CO_2 concentration from 60 to 20 kyr BP from the Taylor Dome ice core, Antarctica. Geophys. Res. Lett. 27 (5), 735–738.

Jonkers, L., Moros, M., Prins, M.A., Dokken, T., Andersson Dahl, C, Dijkstra, N., Perner, K., Brummer, G.-J.A., 2010a. A reconstruction of sea surface warming in the northern North Atlantic during MIS 3 ice-rafting events. Quat. Sci. Rev. 29, 1791–1800.

Jonkers, L., Brummer, G.-J.A., Peters, F.J.C., van Aken, H.M.I., DeJong, M.F., 2010b. Seasonal stratification, shell flux and oxygen isotope dynamics of left-coiling *N. pachyderma* and *T. quinqueloba* in the western subpolar North Atlantic. Paleoceanography 25 (PA2204). doi:10.1029/2009PA001849.

King, J.W., Banerjee, S.J., Marvin, J., 1983. A new rock-magnetic approach to selecting sediments for geomagnetic paleointensity studies: application to paleointensity for the last 4000 years. J. Geophys. Res. 88, 5911–5921.

Kissel, C., Laj, C., Mulder, T., Wandres, C., Cremer, M., 2009. The magnetic fraction: a tracer of deep water circulation in the North Atlantic. Earth Planet. Sci. Lett. 288, 444–454.

Kissel, C., Laj, C., Piotrowski, A.M., Goldstein, S.L., Hemming, S.R., 2008. Millennial-scale propagation of Atlantic deep waters to the glacial Southern ocean. Paleoceanography 23 (PA2102). doi:10.1029/2008PA001624.

Knorr, G., Lohmann, G., 2007. Rapid transitions in the Atlantic thermohaline circulation triggered by global warming and meltwater during the last deglaciation. Geochem. Geophys. Geosyst. 8 (12). doi:10.1029/2007GC001604.

Knutti, R., Flückiger, J., Stocker, T.F., Timmermann, A., 2004. Strong hemispheric coupling of glacial climate through freshwater discharge and ocean circulation. Nature 420, 851–856.

Lacasse, C., Carey, S., Sigurdsson, H., 1998. Volcanogenic sedimentation in the Iceland Basin: influence of subaerial and subglacial eruptions. J. Volcanol. Geoth. Res. 83, 47–73.

Lacasse, C., Sigurdsson, H., Johannesson, H., Paterne, M., Carey, S., 1995. Source of ash zone 1 in the north Atlantic. Bull. Volcanol. 57, 18–32.

Lisiecki, L.E., Raymo, M.E., 2005. A Pliocene-Pleistocene stack of 57 globally distributed benthic δ^{18}O records. Paleoceanography 20 (PA1003). doi:10.1029/2004PA001071.

Liu, Z., Otto-Bleisner, B.L., He, F., Brady, E.C., Tomas, R., Clark, P.U., Carlson, A.E., Lynch-Stieglitz, J., Curry, W., Brook, E., Efickson, D., Jacob, R., Kutzbach, J., Cheng, J., 2009. Transient simulation of last deglaciation with a new mechanism for Bølling-Allerød warming. Science 325, 310–314.

Löwemark, L., Grootes, P.M., 2004. Large age differences between planktic foraminifers caused by abundance variations and Zoophycos bioturbation. Paleoceanography 19, PA2001. doi:10.1029/2003PA000949.

Löwemark, L., Konstantinou, K.I., Steinke, S., 2008. Bias in foraminiferal multispecies reconstructions of paleohydrographic conditions caused by foraminiferal abundance variations and bioturbational mixing: a model approach. Mar. Geol. 256, 101–106.

Martrat, B., Grimalt, J.O., Shackleton, N.J., de Abreu, L., Hutterli, M.A., Stocker, T.F., 2007. Four climate cycles of recurring deep and surface water destabilizations on the Iberian Margin. Science 317, 502–507.

McManus, J.F., Bond, G.C., Broecker, W.S., Johnsen, S., Labeyrie, L., Higgins, S., 1994. High-resolution climate records from the North Atlantic during the Last Interglacial. Nature 371, 326–329.

Meese, D.A., Alley, R.B., Gow, A.J., Grootes, P., Mayewski, P.A., Ram, M., Taylor, K.C., Waddington, E.D., Zielinski, G., 1994. Preliminary Depth-age Scale of the GISP2 Ice Core. CRREL, Special Report, 94-1, 66 pp.

Mignot, J., Ganopolski, A., Levermann, A., 2007. Atlantic subsurface temperatures: response to a shutdown of the overturning circulation and consequences for its recovery. J. Clim. 20 (9), 4884–4898.

Mix, A.C., Ruddiman, W.F., McIntyre, A., 1986. Late Quaternary paleoceanography of the tropical Atlantic, 1: spatial variability of annual mean sea-surface temperatures, 0–20,000 years B.P. Paleoceanography 1, 43–66.

Moros, M., Kuijpers, A., Snowball, I., Lassen, S., Backstrom, D., Gingele, F., McManus, J., 2002. Were glacial iceberg surges in the North Atlantic triggered by climatic warming? Mar. Geol. 192, 393–417.

Piotrowski, A.M., Goldstein, S.L., Hemming, S.R., Fairbanks, R.G., Zylberberg, D.R., 2008. Oscillating glacial northern and southern deep water formation from combined neodymium and carbon isotopes. Earth Planet. Sci. Lett. 272, 394–405.

Pisias, N.G., Clark, P.U., Brook, E.J., 2010. Modes of climate variability during Marine Isotope Stage 3 (60–26 ka). J. Clim. 23, 1581–1588.

Prins, M.A., Troelstra, S.R., Kruk, R.W., van der Borg, K., de Jong, A.F.M., Weltje, G.J., 2001. The late Quaternary sedimentary record of Reykjanes Ridge, north Atlantic. Radiocarbon 43, 939–947.

Rashid, H., Boyle, E.A., 2007. Mixed-layer deepening during Heinrich events: a multi-planktonic foraminiferal δ^{18}O approach. Science 320, 439–441.

Richter, T.O., van der Gaast, S., Koster, B., Vaars, A., Gieles, R., de Stigter, H.C., DeHaas, H., van Weering, T.C.E., 2006. The Avaatech XRF Core Scanner: Technical Description and Applications to NE Atlantic Sediments. In: Geological Society, London, Special Publications, vol. 267, pp. 39–50.

Robinson, S.G., Maslin, M.A., McCave, I.N., 1995. Magnetic susceptibility variations in upper Pleistocene deep-sea sediments of the NE Atlantic: implications for ice rafting and paleocirculation at the last glacial maximum. Paleoceanography 10, 221–250.

Rohling, E.J., Grant, K., Hemleben, C., Kucera, M., Roberts, A.P., Schmeltzer, I., Schulz, H., Siccha, M., Siddall, M., Trommer, G., 2008. New constraints on the timing of sea level fluctuations during early to middle marine isotope stage 3. Paleoceanography 23 (PA3219). doi:10.1029/2008PA001617.

Rohling, E.J., Marsh, R., Wells, N.C., Siddall, M., Edwards, N.R., 2004. Similar meltwater contributions to glacial sea level changes from Antarctic and northern ice sheets. Nature 430, 1016–1021.

Ruddiman, W.F., 1977. Late Quaternary deposition of ice-rafted sand in the subpolar North Atlantic (lat 40° to 65°N). Geol. Soc. Am. Bull. 88, 1813–1827.

Schmittner, A., Yoshimori, M., Weaver, A.J., 2002. Instability of glacial climate in a model of the ocean-atmosphere-cryosphere system. Science 295, 1489–1493.

Shackleton, N.J., Fairbanks, R.G., Chiu, T.-C., Parrenin, F., 2004. Absolute calibration of the Greenland time scale: implications for Antarctic time scales and for Δ^{14}C. Quaternary Sci. Rev. 23, 1513–1522.

Shackleton, N.J., Hall, M.A., Vincent, E., 2000. Phase relationships between millennial-scale events 64,000–24,000 years ago. Paleoceanography 15 (6), 565–569.

Shaffer, G., Olsen, S.M., Bjerrum, C.J., 2004. Ocean subsurface warming as a mechanism for coupling Dansgaard–Oeschger climate cycles and ice-rafting events. Geophys. Res. Lett. 31 (L24202). doi:10.1029/2004GL020968.

Siddall, M., Rohling, E.J., Thompson, W.G., Waelbroeck, C., 2008. MIS 3 Sea-level fluctuations: data synthesis and new outlook. Rev. Geophys. 46 (RG4003). doi:10.1029/2007RG000226.

Siddall, M., Rohling, E.J., Almogi-Labin, A., Hemleben, Ch., Meischner, D., Schmelzer, I., Smeed, D.A., 2003. Sea-level fluctuations during the last glacial cycle. Nature 423, 853–858.

Sierro, F.J., Andersen, N., Bassetti, M.A., Berne, S., Canals, M., Curtis, J.H., Dennielou, B., Flores, J.A., Figola, J., Gonzalez-Mora, B., Grimalt, J.O., Hodell, D.A., Jouet, G., Perez-Folgado, M., Schneider, R., 2009. Quaternary Sci. Rev. 28, 1–15.

Skinner, L.C., 2008. Revisiting the absolute calibration of the Greenland ice-core age-scales. Clim. Past Discuss. 4, 791–807.

Skinner, L.C., Elderfield, H., 2007. Rapid fluctuations in the deep North Atlantic heat budget during the last glacial period. Paleoceanography 22 (PA1205). doi:10.1029/2006PA001338.

Skinner, L.C., Elderfield, H., Hall, M., 2007. Phasing of millennial events and Northeast Atlantic deep-water temperature change since 50 ka BP. In: Ocean Circulation: Mechanisms and Impacts – Past and Future Changes of Meridonial Overturning. AGU, Washington D.C., pp. 197–208.

Skinner, L.C., Shackleton, N.J., Elderfield, H., 2003. Millennial-scale variability of deep-water temperature and $\delta^{18}O_{dw}$ indicating deep-water source variations in the Northeast Atlantic, 0–34 cal. ka BP. Geochem. Geophys. Geosyst. 4 (12), 1098. doi:10.1029/2003GC000585.

Smethie, W.M., LeBel, D.A., Fine, R.A., Rhein, M., Kieke, D., 2007. Strength and variability of the deep limb of the North Atlantic meridional overturning circulation from chlorofluorocarbon inventories. In: Schmittner, A., Chiang, J., Hemming, S. (Eds.), Ocean Circulation: Mechanisms and Impacts. Geophysical Monograph Series, vol. 173, pp. 119–130.

Steig, E.J., Alley, R.B., 2002. Phase relationships between Antarctic and Greenland climate records. Ann. Glaciol. 35, 451–456.

Stocker, T.F., 1998. The seesaw effect. Science 282, 61–62.

Stocker, T.F., Johnsen, S.J., 2003. A minimum model for the bipolar seesaw. Paleoceanography 18, 1087. doi:10.1029/2003PA000920.

Tauxe, L., 1993. Sedimentary records of relative paleointensity of the geomagnetic field: theory and practice. Rev. Geophys. 31, 319–354.

Thomas, R., Guyodo, Y., Channell, J.E.T., 2003. U-channel track for susceptibility measurements. Geochem. Geophys. Geosyst., 1050. doi:10.1029/2002GC000454.

Thornalley, D.J.R., McCave, I.N., Elderfield, H., 2010. Tephra in deglacial ocean sediments south of Iceland: stratigraphy, geochemistry and oceanic reservoir ages. J. Quat. Sci..

Thouveny, N., Bourles, D.L., Saracco, G., Carcaillet, J.T., Bassinot, F., 2008. Paleoclimatic context of geomagnetic dipole lows and excursions in the Brunhes, clue for an orbital influence on the geodynamo? Earth Planet. Sci. Lett. 275, 269–284.

Van Kreveld, S., Sarnthein, M., Erklenkeuser, H., Grootes, P., Jung, S., Nadeau, M.J., Pflaumann, U., Voelker, A., 2000. Potential links between surging ice sheets, circulation changes and the Dansgaard–Oeschger cycles in the Irminger Sea, 60–18 kyr. Paleoceanography 15 (4), 425–442.

Waelbroeck, C., Labeyrie, L., Michel, E., Duplessy, J.C., McManus, J.F., Lambeck, K., Balbon, E., Labracherie, M., 2002. Sea-level and deep water temperature changes derived from benthic foraminifera isotopic records. Quaternary Sci. Rev. 21, 295–305.

Weltje, G.J., Tjallingii, R., 2008. Calibration of XRF core scanners for quantitative geochemical logging of sediment cores: theory and application. Earth Planet. Sci. Lett. 274, 423–438.

Wunsch, C., 2006. Abrupt climate change: an alternative view. Quaternary Res. 65, 191–203.

Zielinski, G.A., Mayewski, P.A., Meeker, L.D., Gronvold, K., Germani, M.S., Whitlow, S., Twickler, M.S., Taylor, K., 1997. Volcanic aerosol records and tephrochronology of the Summit, Greenland, ice cores. J. Geophys. Res. 102, 26625–26640.